Mine Water and the Environment (2023) 42:687–696
https://doi.org/10.1007/s10230-023-00955-1

TECHNICAL COMMUNICATION

Assessing the Effectiveness of Tailings Pond Seepage Remediation Using the Four Dimensions of "Point-Line-Surface-Body": A Case Study

Shichong Yuan[1] · **Guilei Han**[2,3,4]

Received: 24 May 2023 / Accepted: 12 October 2023 / Published online: 6 November 2023

Abstract

Due to nonstandard anti-seepage facilities, aging failure, and other reasons, some tailings ponds have seepage problems. After analysis of the geological and hydrogeological conditions of a lead–zinc mine tailings pond, an interception, blocking, and drainage (IBD) system engineering scheme was used to comprehensively control the seepage problems there. In addition, we assessed the effectiveness of a grout curtain from the four dimensions of the point-line-surface-body (the 4D of PLSB), including a water pressure test (point), drilling and coring survey (line), geophysical test (surface), and a group-holes pumping test (body). The proposed method provides a comprehensive and accurate understanding of grouting efficiency assessment from the perspectives of permeability and tightness.

Keywords Seepage water · IBD model · Grout curtain · Water pressure tests · ERT · Pumping test

Introduction

The mining and beneficiation of non-ferrous metal and non-metallic deposits generate enormous quantities of solid, liquid, and solid–liquid mixed wastes, including waste rock, tailings water, floating sludge, and smelter slag (Spitz and Trudinger 2008; Yuan et al. 2022a, b). In general, these wastes and tailings are temporarily or permanently stored in tailings ponds. These tailings ponds pose great challenges for ecological and environmental protection and potential geological disasters, such as dam failure, dam overtopping, acid mine drainage, contaminant transport by rainstorms or wind, as well as seepage and runoff of contaminated water (Kemper and Sommer 2002; Romero et al. 2007; Wills and Finch 2015; Yuan et al. 2021).

Long-term seepage from the foundation of a tailings pond dam can seriously pollute rivers, lakes, and groundwater and can cause dam failures and damage to the local ecological and geological environment (Heikkinen et al. 2009; Shakhane et al. 2022; Sheoran and Sheoran 2006). Rey et al. (2021) verified that the combined use of electrical resistivity tomography (ERT) and induced polarisation (IP) methods were effective for monitoring the structural characteristics of tailings dams and assessing the leachate contamination area. Shakhane et al. (2022) showed that internal erosion within the embankment was a major reason for many tailings dam failures and delineated two prominent anomalies within such an embankment in the Letšeng Diamond Mine's two tailings ponds by resistivity survey. Buselli and Lu (2006) investigated the seepage problems at the Ranger tailings pond in the Northern Territory, Australia using a combination of geophysical methods (direct current resistivity, self-potential, induced polarisation, and transient electromagnetic) and presented an optimal combination of these methods for long-term monitoring of potential seepage. Of the geophysical survey methods used to date, direct current resistivity and electromagnetic geophysical survey methods are sensitive

✉ Shichong Yuan
yuanshichong@cumt.edu.cn

Guilei Han
498822793@qq.com

1 School of Resources and Geosciences, China University of Mining and Technology, 1 University Rd., Xuzhou 221116, Jiangsu, China

2 School of Mechanics and Civil Engineering, China University of Mining and Technology, Xuzhou 221116, Jiangsu, China

3 North China Engineering Investigation Institute Co., Ltd., Shijiazhuang 050021, Hebei, China

4 Technology Innovation Center for Groundwater Disaster Prevention and Control Engineering for Metal Mines, Ministry of Natural Resources, 39 Huitong Rd., Shijiazhuang 050021, Hebei, China

to the resistivity of the subsurface discontinuities, while the results of induced polarisation and self-potential methods are affected by the electrochemical properties of the ground as well as its resistivity. Therefore, the induced polarisation and electrical resistivity tomography methods are the most effective for use in the detection of seepage areas with high chargeability values consistently observed over the known seepage path and the contaminated area (Buselli and Lu 2006; Rey et al. 2021; Gao et al. 2018).

Curtain grouting is one of the most effective ways to block underground water seepage pathways and reinforce soil and rock masses, especially in the field of underground mining and dam foundation (Bonacci and Roje-Bonacci 2012; Gao and Han 2021; Rombough et al. 2017; Yuan and Han 2020). The main methods used to assess the effectiveness of grout curtain include theoretical analysis, numerical simulation, modeling, and geophysical surveys. In practical engineering, water pressure test are the most popular and effective method of determining the permeability of rock masses in curtain grouting efficiency assessment (Huang et al. 2016; Sadeghiyeh et al. 2013). Other in situ tests such as acoustic velocity tests, coring and drilling, borehole television imaging, and seismic tests also have been commonly used to evaluate the improvement of rock masses in grouting (Chen et al. 2015; Han et al. 2015; Lynch et al. 2012). Zhu et al. (2019) proposed a cloud-model-based fuzzy comprehensive assessment method for grout curtain effectiveness, which considered the permeability and compactness of the rock mass and the fuzziness and randomness of the grouting process. Chen et al. (2021) used large-scale pumping tests on site and groundwater numerical simulation based on FEFLOW to evaluate the water inflow at an iron mine surrounded by an imperfect grout curtain. Yuan et al. (2022a, b) used cross-hole resistivity tomography to determine grouting effectiveness in the Zhongguan iron mine; the results indicated that the grouting had obviously improved the continuity and strength of the surrounding rocks. Zhou et al. (2017) established a microseismic monitoring system to access the potential seepage pathways of a grout curtain in the Zhangmatun iron mine due to the influence of multiple factors including inadequate grouting area, weak rock, and mining disturbance. Battaglia et al. (2016) located the seepage zones in a grout curtain in the Bumbuna dam using fluorescent tracer tests and achieved great success. The effectiveness of grout curtain have also been assessed using pump tests, hydrochemistry, and electrical conductivity (Chegbeleh et al. 2019; Huang et al. 2019; Wieland and Kirchen 2012).

However, assessing the effectiveness of a grout curtain from a single dimension or with a single method cannot fully reflect the actual situation. Comprehensive assessment of grout curtains is a great challenge worldwide and is important for prevention and remediation of seepage failures in tailings ponds. This paper presents a case study on assessing the effectiveness of a grout curtain in a mine tailings pond based on the four dimensions of "point-line-surface-body". The methodology used included a water pressure test (point), a drilling and coring survey (line), a geophysical test (surface), and a group-holes pumping test (body), to comprehensively and systematically evaluate the effectiveness of grouting, effectively avoiding the shortcomings of a single evaluation method.

Geological Background and Seepage Problem

The Study Area

The studied tailings pond is used to store waste lead–zinc tailings slurry from mineral processing plant no. 3 operated by Rongda Mining Co., Ltd. in the Xin Barag Right Banner of northeast Inner Mongolia, China. The detailed location of the studied tailings pond is shown in Fig. 1, which is a border region of China, Russia, and Mongolia. The climate of Xin Barag Right Banner is a mid-temperate continental arid climate with four distinct seasons. The proven mineral resources in the Xin Barag Right Banner include metals such as lead, zinc, gold, silver, copper, and non-metallic minerals such as petroleum, coal, mirabilite, agate, silica, and fluorite. The average annual rainfall is about 243.9 mm with an average annual evaporation of 1572.2 mm. As the Xin Barag Right Banner is controlled by the Mongolian high pressure in winter, the winds are dominantly from the northwest, and the ecological environment is extremely fragile.

Engineering and Hydrogeological Conditions

The auxiliary dam of the tailings pond is a rockfill dam with a maximum dam crest elevation of 813.5 m and a maximum dam height of 21.5 m. The primary dam was built at one time, and the auxiliary dam of each stage was built by heightening in stages. The current dam body is the Phase I dam body with a dam crest elevation of 806.5 m. The Phase II dam is built on the outer slope of the Phase I dam and has a final crest elevation of 813.5 m. An engineering and hydrogeological survey were carried out along the auxiliary dam to provide a targeted, detailed seepage remediation plan. According to the geological survey data, plain fill, humus, brecciated clay, volcanic breccia, and andesite strata are mainly distributed in the study area, in that order, from top to bottom. The physical mechanics and permeability properties of each strata (dam foundation) in the study area are listed in supplemental Table S-1. The quality grade of the rock mass in supplemental Table S-1 is classified according to the "Standard for Engineering Classification of Rock Mass" (GB/T50218-2014; Ministry of Water Resources

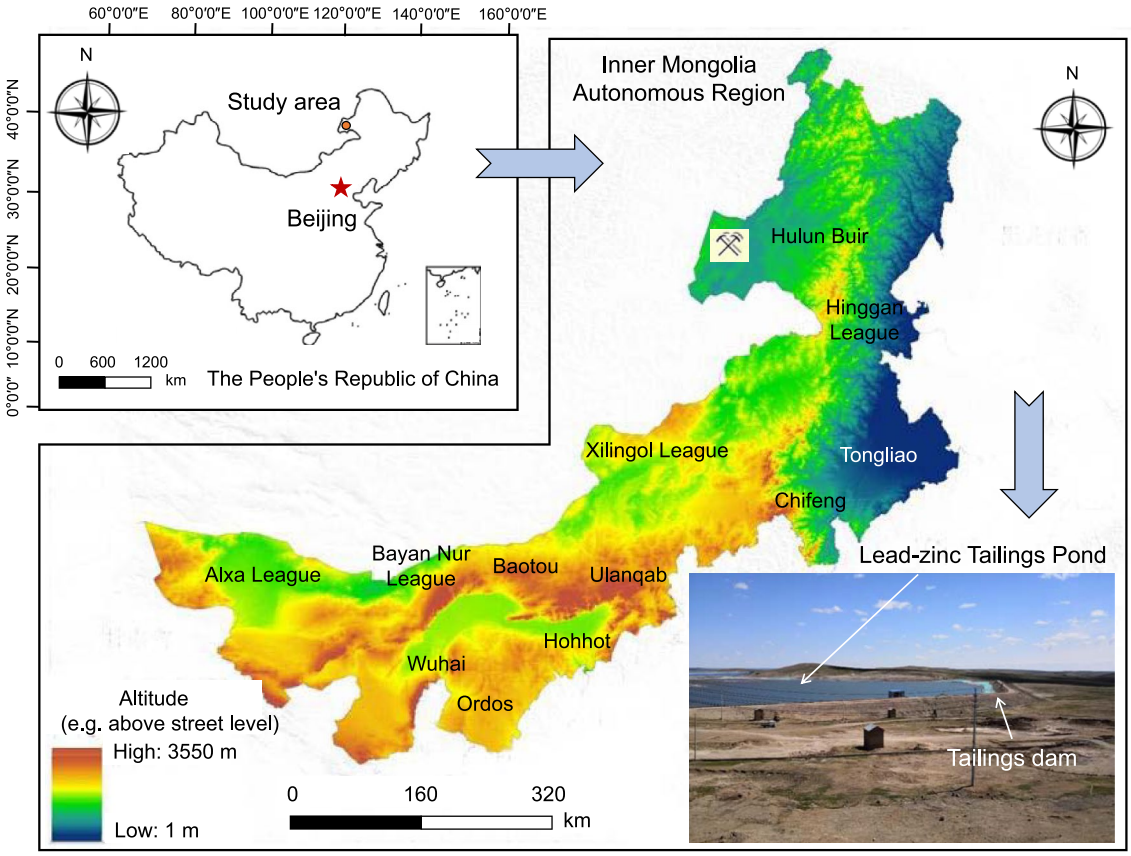

Fig. 1 Location of the study area

of the People's Republic of China 2014). The permeability grade in supplemental Table S-1 is classified according to the "Code for Engineering Geological Investigation of Water Resources and Hydropower" (GB 50487–2008; Ministry of Water Resources of the People's Republic of China 2022). The groundwater of the study area is mainly recharged by vertical infiltration of atmospheric precipitation and upstream lateral infiltration. The runoff of groundwater is mainly controlled by the topographic conditions and rock mass joints and fractures. The buried depth of the stable groundwater level is 0.2–13.5 m, which is equivalent to the elevation of 792.7–808.3 m. The groundwater is mainly stored in Quaternary and broken strongly weathered bedrock.

Seepage Problem of Mine Tailings Pond

At present, for tailings pond with seepage, the conventional remediation method is to cut off the groundwater flow path by installing an underground vertical impervious body downgradient of the tailings pond (Fu et al. 2021; Yang et al. 2020; Yuan et al. 2022a, b). During the Phase II dam foundation clearing, contaminated water seepage from the mine tailings pond was found to be emerging at the foot of the auxiliary dam (Fig. 2). Because the shallow Quaternary and strongly weathered strata have medium and strong permeability, the seepage water did not appear on the surface, but flowed downgradient through the underground aquifer (Fig. 3a). If effective engineering remediation measures are not taken in time, the metal pollutants contained in the seepage water will have an adverse impact on the fragile groundwater ecological environment downstream of the study area.

Methodology

Controlling the Seepage Water

Based on a comprehensive analysis of the geological conditions and remediation requirements, we determined that the seepage problem could not be solved simply by blocking. Because the water head of the tailings pond was higher than the surface elevation of the area, water blocked by an impervious body in the flow path was bound to overflow the surface or overflow the top of the impervious body to the downstream area. To solve this problem, the system engineering scheme of interception, blocking and drainage (IBD) was designed to control the tailings pond seepage water (Fig. 3b

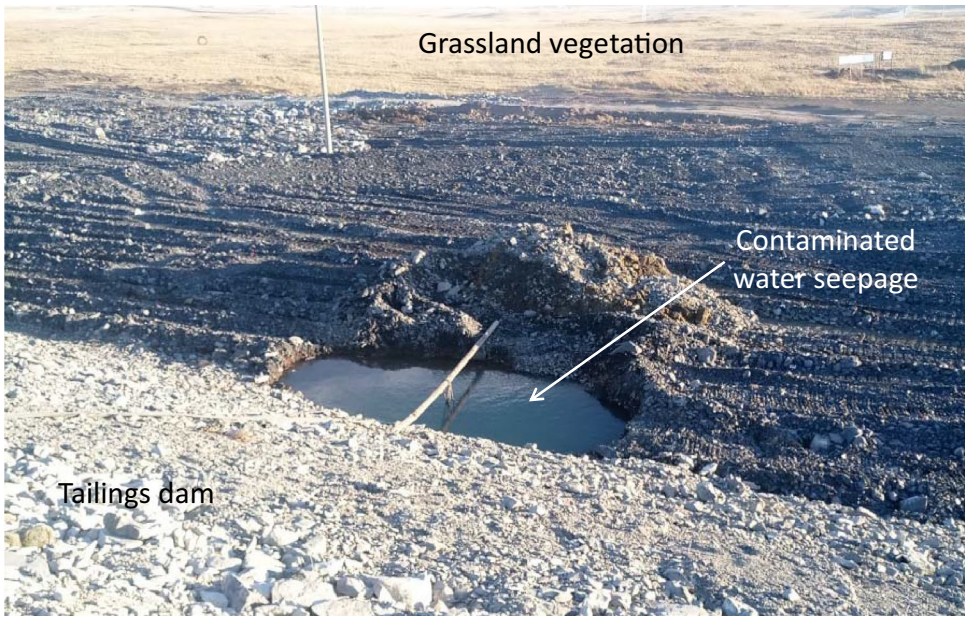

Fig. 2 Contaminated water seepage at the foot of the tailings dam

and c). Interception refers to the excavation of an intercepting ditch along the dam toe, which was filled with gravel to intercept the shallow seepage water. Blocking refers to the construction of an underground impervious body downgradient of the intercepting ditch at the dam toe. The bottom boundary and two shoulders of the impervious body must prevent the seepage from migrating to the downgradient area. Drainage refers to an array of liquid collection wells constructed in the low-lying and highly permeable areas to collect the seepage water along the intercepting ditch; this water can be pumped back to the tailings pond for beneficiation and utilization, to avoid the surface overflow of the seepage water.

According to the characteristics of the rock and soil layer in the study area, the shallow loose layer and completely weathered bedrock could not be effectively grouted, but it proved suitable for incorporation into a poured concrete wall. Additionally, curtain grouting was used for the fissured bedrock to block the deep seepage pathways; the detailed design scheme is shown in Fig. 3b and c. The impervious concrete wall is 0.6 m thick, has an average depth of about 7 m, and a strength grade of C20. The curtain grouting drilling holes were arranged in two rows, distributed along both sides of the concrete wall, with a row spacing of 0.6 m and a drilling hole spacing of 1.5 m. The two rows of drilling holes are staggered (Fig. 3c). The depth of the curtain grouting bottom boundary entering the relative water-resisting layer was at least 5.0 m. The average depth of the grout curtain drilling hole was about 50 m. The designed intercepting ditch was 1.0 m wide and 2.0 m deep and was filled with pea gravel as a filter layer. A total of eight liquid collecting wells were constructed, and the diameter of the liquid collecting well was required to be at least 0.8 m. A 426 mm diameter filter tube was placed inside, and the annular gap between the filter tube and the hole wall was filled with pea gravel as the filter layer. Photographs of the on-site construction are shown in Fig. 3d and e.

Assessing the Effectiveness of a Grout Curtain

Assessing the effectiveness of a grout curtain is an important step in verifying its long-term water blocking effect (Daniels et al. 2000; Fan et al. 2016; Yuan and Han 2020). However, it can be very difficult to comprehensively assess the effectiveness of a grout curtain. Currently, the assessment methods are mostly based on single-dimensional analysis, for example water level or water quality change, drilling and coring surveys, geophysical surveys, in-situ water pressure tests, numerical simulation, and so on, which cannot accurately and comprehensively estimate the implementation. This paper will assess the effectiveness of a grout curtain from the point, line, surface and body dimensions (4D of PLSB), including a water pressure test (point), a drilling and coring survey (line), a geophysical test (surface), and a group holes pumping test (body). Among these, the water pressure and group holes pumping tests can be used to estimate the grouting efficiency from the perspectives of permeability, while drilling and coring surveys and geophysical tests can estimate the grouting efficiency from the perspective of tightness. The proposed method provides a comprehensive and accurate understanding of grouting efficiency.

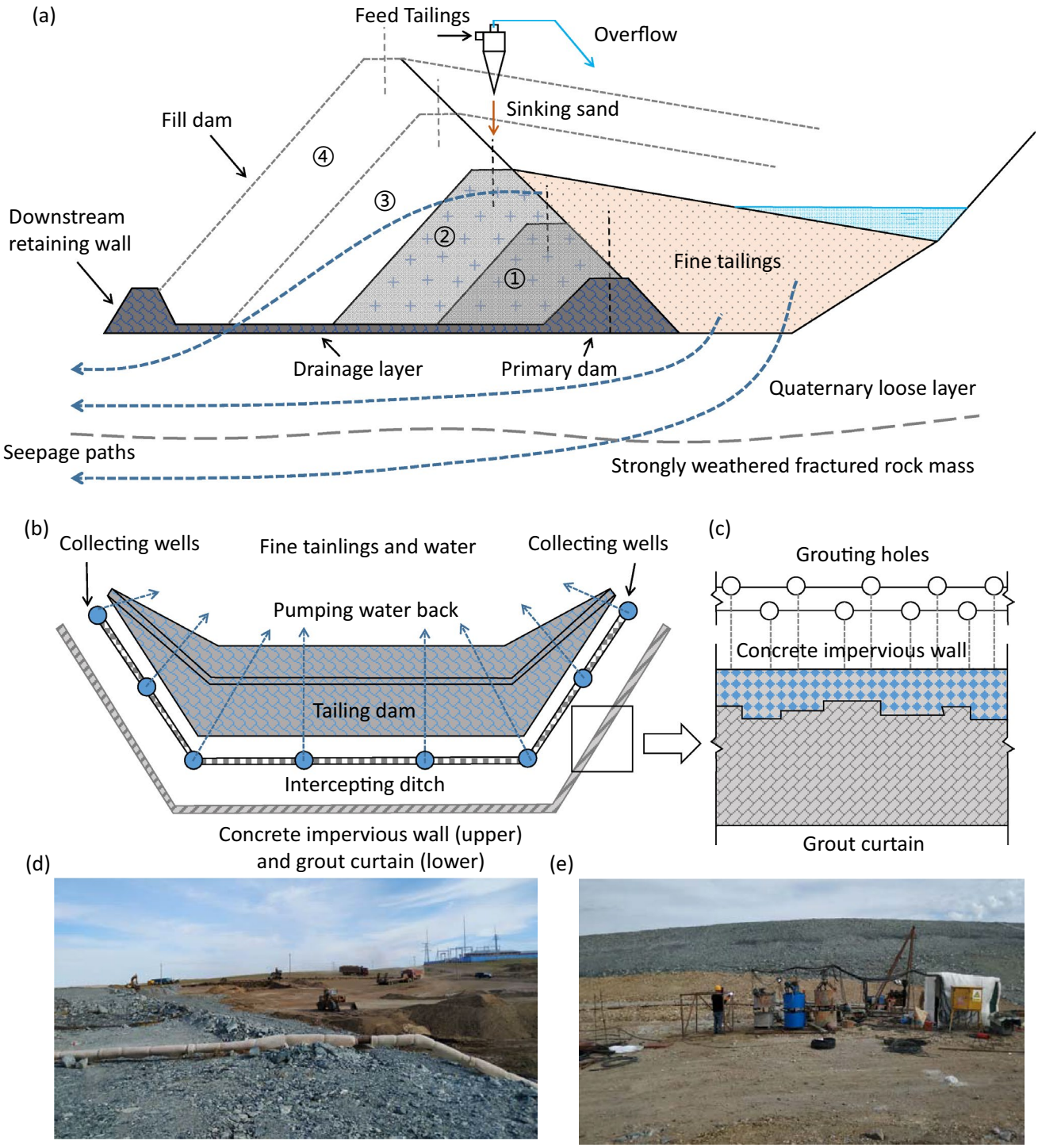

Fig. 3 Using the IBD model to remediate a tailings pond seepage problem. **a** Tailings dam structure and seepage paths. **b** Design plan of IBD model. **c** Design cross section of IBD model. **d** Construction site. **e** Grouting station

Results and Discussion

Water Pressure Tests—Point Dimension

Water pressure tests are extensively used to determine rock mass permeability in curtain grouting assessments (Zadhesh et al. 2014; Magoto 2014; Roman et al. 2013). In situ water pressure testing over discrete zones in drilled holes provides a method to verify the effectiveness of grouting. Each grouting borehole is divided into several 5–10 m long sections for grouting. A water pressure test is required after completely grouting each section at a water pressure of about 80% of the grouting pressure. The injection flow rate is measured every 3–5 min. When the difference between the maximum and minimum values in five consecutive flows is less than 10% of the final value or when the difference between the maximum and minimum values is less than 1.0 L/min, the test can be ended, and the final value used as the calculated value (The Industry Standard Editorial Committee of the People's Republic of China 2015). Supplemental Fig. S-1 shows the device used to conduct a water pressure test in a borehole. The permeability rate can be calculated by Formula (1).

$$q = \frac{Q}{PL} \tag{1}$$

where q is the permeability rate, in Lu; Q is the water reinjection flow, in L/min; P is the water pressure, in MPa; and L is the length of the test section, in m.

Table 1 shows the water pressure test results for inspection drilling holes 1J1–30J1. The maximum permeability rate for these drilling holes was less than 2.0 Lu, indicating that the grouting effectiveness of the test section was good (The Industry Standard Editorial Committee of the People's Republic of China 2015). The location of inspection drilling holes 1J1–30J1 is shown in Fig. 4a, and two representative borehole histograms (5J1 and 28J1), with the lithology and permeability rate shown in Fig. 4b and c, respectively. However, the water pressure test results only reflect the permeability of a certain section of the drilling hole, and so have certain limitations.

Drilling and Coring Survey—Line Dimension

Drilling and coring surveys are an effective way to observe the development of bedrock fractures and the effect of slurry diffusion (Dou et al. 2020; Fan et al. 2016). Due to the heterogeneous diffusion of slurry in the bedrock fractures under grouting pressure, some wide and large fractures can be effectively filled by slurry, while some thin and small fractures cannot (Zhang 2022). Figure 5 shows the core specimen images of selected typical drilling holes. It can be seen from Fig. 5 that the grout slurry fully filled the bedrock joints and fissures, solidified fully, and the setting rate was high. The broken zone is fully cemented by the grout slurry, which indicates that the grout curtain is continuous and complete, and the waterproof effect is good. However, drilling and coring survey only provide a one-hole view and cannot comprehensively reflect the overall water blocking effect of grout curtain.

Table 1 Test results of water pressure test of inspection drilling holes

Test holes	Depth (m)	Maximum permeability rate (Lu)	Test holes	Depth (m)	Maximum permeability rate (Lu)
1J1	46.68	1.21	16J1	61.8	1.34
2J1	46.91	1.47	17J1	68.22	1.24
3J1	54.57	1.19	18J1	51.15	1.23
4J1	49.71	1.08	19J1	46.43	1.32
5J1	43.30	1.23	20J1	47.06	1.48
6J1	49.06	1.29	21J1	56.29	1.32
7J1	55.54	1.28	22J1	54.57	1.54
8J1	55.67	1.24	23J1	49.59	1.39
9J1	59.43	1.09	24J1	64.48	1.19
10J1	61.93	1.47	25J1	60.84	1.14
11J1	56.7	1.32	26J1	54.49	1.12
12J1	54.28	1.57	27J1	59.29	1.23
13J1	54.53	1.34	28J1	57.44	1.22
14J1	51.9	1.50	29J1	58.94	1.32
15J1	51.73	1.19	30J1	52.35	1.73

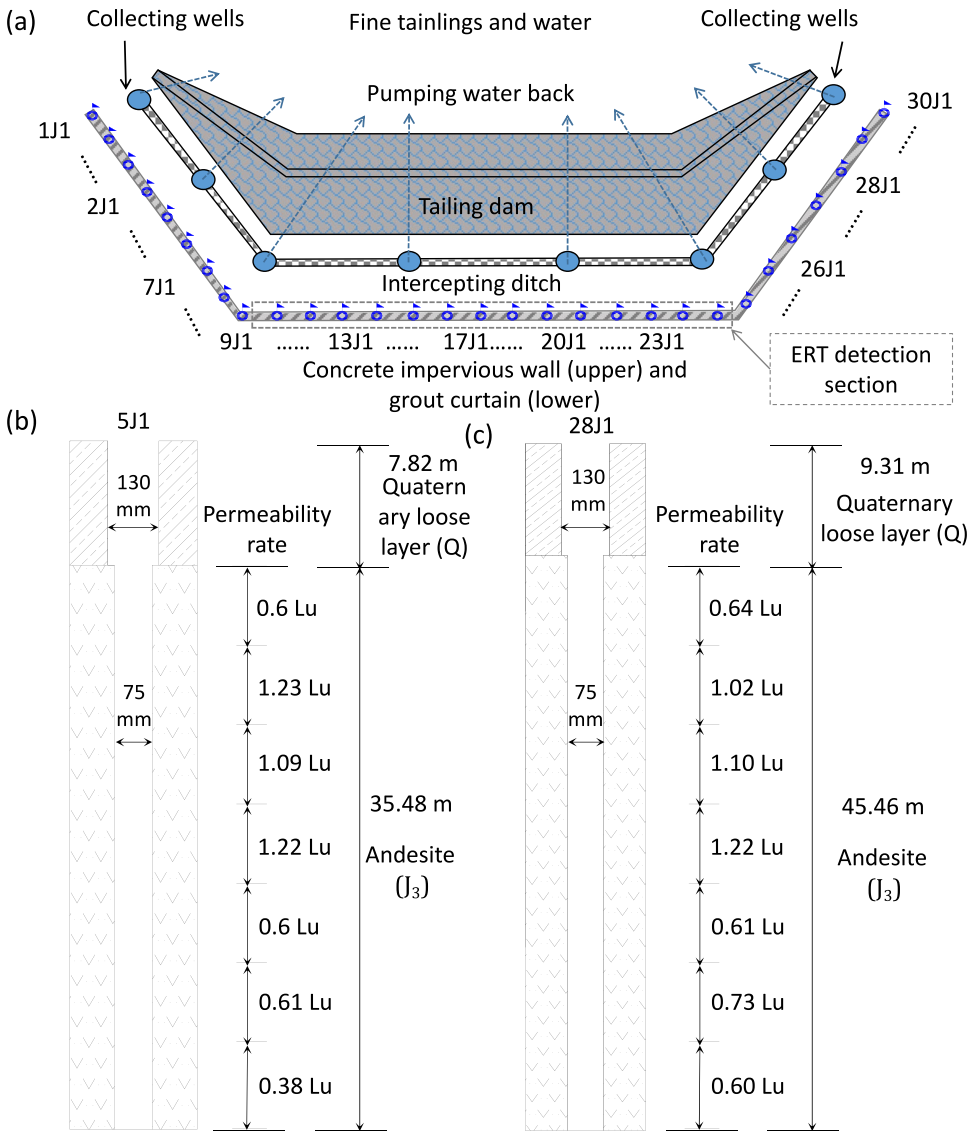

Fig. 4 **a** Location of the inspection drilling holes 1J1–30J1. **b** Two representative borehole histograms (5J1 and 28J1) with lithology and permeability rate

Electrical Resistivity Tomography—Surface Dimension

Electrical resistivity tomography (ERT) can describe geologic bodies by varying electrode spacing in detail over different scales and is widely applied in engineering geology projects (Gao et al. 2018). Figure 6a and b shows the ERT detection results before and after curtain grouting. The metal pollution halo clearly moves deeper along one pollution channel, while the shallow pollution halo is decreasing. The concrete wall (the upper part) and grout curtain (the lower part) successfully blocks the auxiliary dam seepage water, and the grouting effectiveness is relatively obvious.

Group Holes Pumping Test—Body Dimension

To verify the influence scope of the pumping test, a large-diameter pumping hole, S2, was drilled in the key impervious section, and three observation holes (G4, G5, and G6) were drilled at an equal distance around S2 to analyse the influence of the pumping test in each direction and evaluate the effectiveness of the concrete wall (upper part) and grout curtain (lower part). GC-3 is an observation hole located inside the grout curtain. Supplemental Fig. S-2 shows the distribution of the pumping hole and observation holes. The water level response of each observation hole is shown in Table 2; when the flow of the pumping

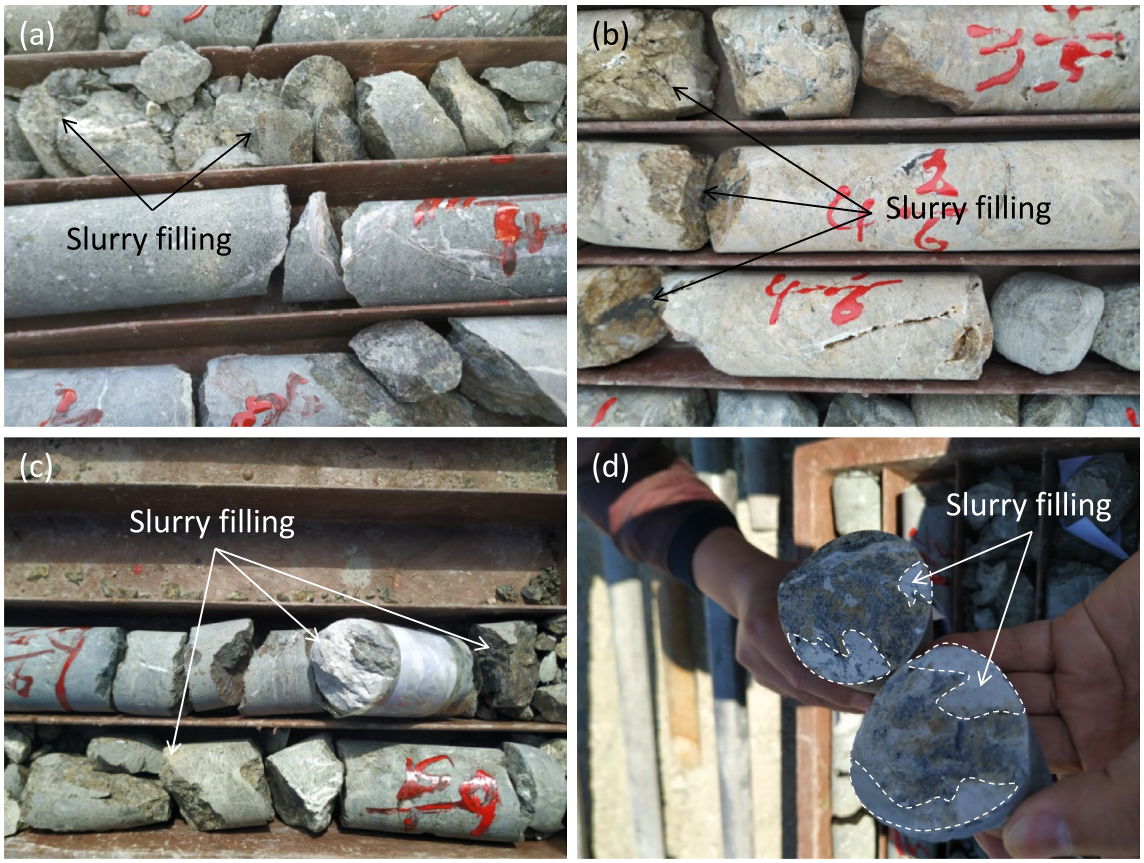

Fig. 5 Core specimen images of the selected typical drilling holes

hole S2 was 5.67 m^3/h, the water level drop is 10.63 m. It can be seen from Table 2 that the water level in the observation holes located inside the grout curtain changed very little despite obvious water level changes in the observation holes outside of the grout curtain. This shows that the grout curtain forms a relatively impermeable boundary in the tailings pond leakage area.

Limitations and Further Study

The focus of this study was to demonstrate successful remediation of a seepage tailings pond in an area of fragile groundwater ecosystems. The seepage water remediation method and the way in which the effectiveness of the grout curtain was assessed can be useful tailings pond with similar geologic and hydrogeological conditions, though it is necessary to adjust the drilling layout, grouting materials, and pressure based on actual site requirements.

Conclusion

This paper presents a typical case of tailings pond seepage remediation and a way to assess its effectiveness. By systematically analyzing the engineering and hydrogeological conditions of the study area, the IBD system engineering scheme was used to comprehensively control the seepage problem. In addition, we assessed the effectiveness of the grout curtain from the four dimensions of PLSB. The water pressure test results show that the maximum permeability rate of inspection drilling holes was less than 2.0 Lu. The grout slurry fully filled the bedrock joints and fissures, solidified fully, and set well. The ERT detection results show that the metal pollution halo moved deeper along one pollution channel, while the shallow pollution halo decreased. The water level response inside and outside the grout curtain fully proves that the grout curtain forms a relatively impermeable boundary in the tailings pond leakage area. The assessment results show that the IBD approach is a very effective way to remediate tailings

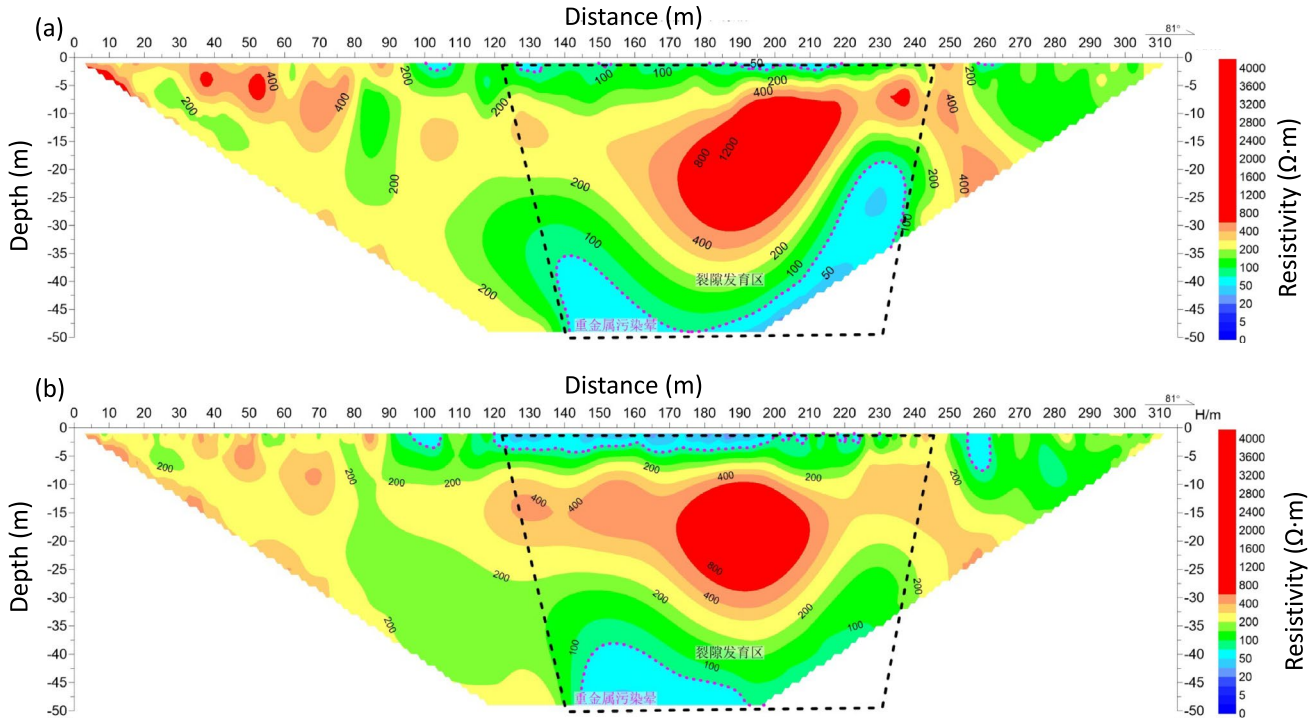

Fig. 6 ERT detection results before and after curtain grouting. **a** Before curtain grouting. **b** After curtain grouting

Table 2 Water level response of each observation hole

Observation holes	Distance with S2 (m)	Initial water level buried depth (m)	Stable water level buried depth (m)	Water level change (m)
GC03	15	1.52	1.55	0.03
GC11	3	3.82	6.06	2.24
G4	15	4.10	4.52	0.42
G5	15	4.23	5.04	0.81
G6	15	3.62	4.38	0.76

pond seepage and could likely be useful at other tailings ponds.

Supplementary Information The online version contains supplementary material available at https://doi.org/10.1007/s10230-023-00955-1.

Acknowledgements The authors acknowledge the financial support of the Key Research and Development Program of Hebei Province under Grant 21373901D. The authors thank Weiqiang Duan, Weixin Li and Jiansong Shi of North China Engineering Investigation Institute Co., Ltd. for their assistance and guidance in the hydrogeological investigation and geological background.

References

Battaglia D, Birindelli F, Rinaldi M, Vettraino E, Bezzi A (2016) Fluorescent tracer tests for detection of dam leakages: the case of the Bumbuna dam - Sierra Leone. Eng Geol 205:30–39. https://doi.org/10.1016/j.enggeo.2016.02.010

Bonacci O, Roje-Bonacci T (2012) Impact of grout curtains on karst groundwater behaviour: an example from the Dinaric karst. Hydrol Process 26(18):2765–2772. https://doi.org/10.1002/hyp.8359

Buselli G, Lu KL (2006) Groundwater contamination monitoring with multichannel electrical and electromagnetic methods. J Appl Geophys 48(1):11–23. https://doi.org/10.1016/S0926-9851(01)00055-6

Chegbeleh LP, Akabzaa TM, Akudago JA, Yidana SM (2019) Investigation of critical hydraulic gradient and its application to the design and construction of bentonite-grout curtain. Environ Earth Sci 78:370. https://doi.org/10.1007/s12665-019-8367-0

Chen M, Lu WB, Zhang WJ, Yan P, Zhou CB (2015) An analysis of consolidation grouting effect of bedrock based on its acoustic velocity increase. Rock Mech Rock Eng 48:1259–1274. https://doi.org/10.1007/s00603-014-0624-7

Chen W, Li W, Wang Q, Qiao W (2021) Evaluation of groundwater inflow into an iron mine surrounded by an imperfect grout curtain. Mine Water Environ 40(2):520–538. https://doi.org/10.1007/s10230-021-00777-z

Daniels JL, Chien CC, Ogunro VO, Inyang HI (2000) A comparative analysis of contaminant migration models using barrier

material data. J Soil Contam 9(5):487–501. https://doi.org/10.1080/10588330091134365
Dou JX, Zhang GJ, Zhou MX, Wang ZL, Gyatso N, Jiang MQ, Safari P, Liu JQ (2020) Curtain grouting experiment in a dam foundation: case study with the main focus on the Lugeon and grout take tests. Bull Eng Geol Environ 79:4527–4547. https://doi.org/10.1007/s10064-020-01865-0
Magoto Elliot N (2014) Quantifiying the effectiveness of a grout curtain using a laboratory-scale physical model. Univ of Kentucky MS Thesis
Fan GC, Zhong DH, Yan FG, Yue P (2016) A hybrid fuzzy evaluation method for curtain grouting efficiency assessment based on an AHP method extended by D numbers. Expert Syst Appl 44:289–303. https://doi.org/10.1016/j.eswa.2015.09.006
Fu XL, Zhang R, Reddy KR, Li YC, Yang YL, Du YJ (2021) Membrane behavior and diffusion properties of sand/SHMP-amended bentonite vertical cutoff wall backfill exposed to lead contamination. Eng Geol 284:106037. https://doi.org/10.1016/j.enggeo.2021.106037
Gao W, Shi L, Han J, Zhai P (2018) Dynamic monitoring of water in a working face floor using 2D electrical resistivity tomography (ERT). Mine Water Environ 37:423–430. https://doi.org/10.1007/s10230-017-0483-z
Gao X, Han G (2021) Research on applicability and improvement of curtain grouting technology for tailings dam foundation anti-seepage. Nonferrous Metals (min Sect) 73(3):119–123. https://doi.org/10.3969/j.issn.1671-4172.2021.03.018
Han ZQ, Wang C, Zhu H (2015) Research on deep joints and lode extension based on digital borehole camera technology. Pol Marit Res 22:10–14. https://doi.org/10.1515/pomr-2015-0025
Heikkinen PM, Räisänen ML, Johnson RH (2009) Geochemical characterisation of seepage and drainage water quality from two sulphide mine tailings impoundments: acid mine drainage versus neutral mine drainage. Mine Water Environ 28(1):30–49. https://doi.org/10.1007/s10230-008-0056-2
Huang Z, Jiang Z, Zhu S, Wu X, Yang L, Guan Y (2016) Influence of structure and water pressure on the hydraulic conductivity of the rock mass around underground excavations. Eng Geol 202:74–84. https://doi.org/10.1016/j.enggeo.2016.01.003
Huang H, Chen Z, Wang T, Xiang C, Zhang L, Zhou G, Sun B, Wang Y (2019) Nitrate distribution and dynamics as indicators to characterize karst groundwater flow in a mined mineral deposit in southwestern China. Hydrogeol J 27:2077–2089. https://doi.org/10.1007/s10040-019-01987-0
Kemper T, Sommer S (2002) Estimate of heavy metal contamination in soils after a mining accident using reflectance spectroscopy. Environ Sci Technol 36(12):2742–2747. https://doi.org/10.1021/es015747j
Lynch C, Dodson M, McCartney J (2012) Grouting verification using 3-d seismic tomography. In: Proceeding Grouting and Deep Mixing, pp 1506–1515. https://doi.org/10.1061/9780784412350.0126
Ministry of Water Resources of the People's Republic of China (2014) Standard for engineering classification of rock mass (GB/T50218–2014). China Planning Press, Beijing, pp 1–14 (**in Chinese**)
Ministry of Water Resources of the People's Republic of China (2022) Code for engineering geological investigation of water resources and hydropower (GB 50487–2008). China Planning Press, Beijing, pp 116–122 (**in Chinese**)
Rey J, Martínez J, Hidalgo MC, Mendoza R, Sandoval S (2021) Assessment of tailings ponds by a combination of electrical (ERT and IP) and hydrochemical techniques (Linares, southern Spain). Mine Water Environ 40(1):298–307. https://doi.org/10.1007/s10230-020-00709-3
Roman WM, Hockenberry AN, Berezniak JN, Wilson DB, Knight MA (2013) Evaluation of grouting for hydraulic barriers in rock. Environ Eng Geosci 19(4):363–375
Rombough VT, Davies JA, Hoy JP (2017) Grout curtain installation for sump excavation in permafrost region of northern Canada. In: Proceeding 5th International Conference on Grouting, Deep Mixing, and Diaphragm Walls, available at: https://doi.org/10.1061/9780784480786.011
Romero FM, Armienta MA, Gonzalez-Hernandez G (2007) Solid-phase control on the mobility of potentially toxic elements in an abandoned lead/zinc mine tailings impoundment. Appl Geochem 22(1):109–127. https://doi.org/10.1016/j.apgeochem.2006.07.017
Sadeghiyeh SM, Hashemi M, Ajalloeian R (2013) Comparison of permeability and groutability of Ostur Dam site rock mass for grout curtain design. Rock Mech Rock Eng 46:341–357. https://doi.org/10.1007/s00603-012-0282-6
Shakhane T, Nkhumeleni M, Ntokoane M, Makara M (2022) Evaluating seepage through a homogenous embankment: Part of monitoring a tailings storage facility. Mine Water Environ 41(1):103–118. https://doi.org/10.1007/s10230-021-00824-9
Sheoran AS, Sheoran V (2006) Heavy metal removal mechanism of acid mine drainage in wetlands: a critical review. Miner Eng 19(2):105–116. https://doi.org/10.1016/j.mineng.2005.08.006
Spitz K, Trudinger J (2008) Mining and the environment: from ore to metal. CRC Press, New York City
The Industry Standard Editorial Committee of the People's Republic of China (2015) Specification of Mine Curtain Grouting (DZ/T 0285—2015). Geology Press, Beijing, pp 5–12 (**in Chinese**)
Wieland M, Kirchen GF (2012) Long-term dam safety monitoring of Punt dal Gall arch dam in Switzerland. Front Struct Civ Eng 6(1):76–83. https://doi.org/10.1007/s11709-012-0144-z
Wills BA, Finch J (2015) Wills' mineral processing technology: an introduction to the practical aspects of ore treatment and mineral recovery. Elsevier Science, Amsterdam
Yang YL, Reddy KR, Zhang WJ, Fan RD, Du YJ (2020) SHMP-amended Ca-bentonite/sand backfill barrier for containment of lead contamination in groundwater. Int J Env Res Pub He 17(1):370. https://doi.org/10.3390/ijerph17010370
Yuan S, Han G (2020) Combined drilling methods to install grout curtains in a deep underground mine: a case study in southwest China. Mine Water Environ 39(4):902–909. https://doi.org/10.1007/s10230-020-00701-x
Yuan S, Duan W, Liu Y (2021) Effects of recycled fly ash on desiccation cracking of mine tailings with high water content. Arab J Geosci 14:2828. https://doi.org/10.1007/s12517-021-09225-2
Yuan S, Sui W, Han G, Duan W (2022a) An optimized combination of mine water control, treatment, utilization, and reinjection for environmentally sustainable mining: a case study. Mine Water Environ 41(3):828–839. https://doi.org/10.1007/s10230-022-00886-3
Yuan S, Sun B, Han G, Duan W, Wang Z (2022b) Application and prospect of curtain grouting technology in mine water safety management in China: a review. Water 14(24):4093. https://doi.org/10.3390/w14244093
Zadhesh J, Rastegar F, Sharifi F, Amini H, Nasirabad HM (2014) Consolidation grouting quality assessment using artificial neural network (ANN). Indian Geotech J 45(2):136–144. https://doi.org/10.1007/s40098-014-0116-4
Zhang GL (2022) Mechanism of deflection propagation for grouting in fractured rock mass with flowing water and mining effect on grouted curtain: a review. J Eng Geol 30(3):987–997
Zhou JR, Yang TH, Zhang PH, Xu T, Wei J (2017) Formation process and mechanism of seepage channels around grout curtain from microseismic monitoring: a case study of Zhangmatun iron mine, China. Eng Geol 226:301–315. https://doi.org/10.1016/j.enggeo.2017.07.002
Zhu Y, Wang X, Deng S, Zhao M, Ao X (2019) Evaluation of curtain grouting efficiency by cloud model-based fuzzy comprehensive evaluation method. KSCE J Civ Eng 23(7):2852–2866. https://doi.org/10.1007/s12205-019-0519-y